

Beiträge aus der Elektrotechnik

**Jacqueline Damas**

**Cost Optimized Radio-over-Fiber System**

 VOGT

Dresden 2023

Bibliografische Information der Deutschen Nationalbibliothek  
Die Deutsche Nationalbibliothek verzeichnet diese Publikation in der  
Deutschen Nationalbibliografie; detaillierte bibliografische Daten sind im  
Internet über <http://dnb.dnb.de> abrufbar.

Bibliographic Information published by the Deutsche Nationalbibliothek  
The Deutsche Nationalbibliothek lists this publication in the Deutsche  
Nationalbibliografie; detailed bibliographic data are available on the Internet  
at <http://dnb.dnb.de>.

Zugl.: Dresden, Techn. Univ., Diss., 2023

Die vorliegende Arbeit stimmt mit dem Original der Dissertation  
„Cost Optimized Radio-over-Fiber System“ von Jacqueline Damas überein.

© Jörg Vogt Verlag 2023  
Alle Rechte vorbehalten. All rights reserved.

Gesetzt vom Autor

ISBN 978-3-95947-021-6

Jörg Vogt Verlag  
Niederwaldstr. 36  
01277 Dresden  
Germany

Phone: +49-(0)351-31403921  
Telefax: +49-(0)351-31403918  
e-mail: [info@vogtverlag.de](mailto:info@vogtverlag.de)  
Internet : [www.vogtverlag.de](http://www.vogtverlag.de)

Technische Universität Dresden

**Cost Optimized Radio-over-Fiber System**

M. Sc.  
**Jacqueline Damas**

von der Fakultät Elektrotechnik und Informationstechnik der  
Technische Universität Dresden

zur Erlangung des akademischen Grades

**Doktoringenieur**  
(Dr.-Ing.)

genehmigte Dissertation

Vorsitzender: Prof. Dr.-Ing. habil. Frank Ellinger  
Gutachter: Prof. Dr.-Ing. Dirk Plettmeier  
Prof. Nerey Mvungi  
Weiteres Mitglied: Prof. Dr.-Ing. Kambiz Jamshidi

Tag der Einreichung: 15.08.2022  
Tag der Verteidigung: 27.09.2023

# Abstract

The demand of smaller and portable electronic devices has contributed to the realisation of compact embedded systems using PCB miniaturization techniques. The commercial market is faced with competition of handheld users' devices in medical, communication and automotive industries which are smaller and lighter electronic devices. The possibilities of higher degree of integration in planar technology using cost effective electronic components has lead to different art of design and fabrication of compact units.

I this work, a central station and a base station front-end with small form factor have been realized using commercial components on PCBs. These electronic compacts units were integrated in the IF-over-Fiber system architecture. The IF-over-Fiber architecture comprised of miniaturized electronic components for quadrature modulation and upconversion. The central station supports multi-Gbps data rate modulation formats in order to increase the spectral efficiency of the transmitted information. Multilevel modulation formats are considered spectrally efficient and can double the transmission capacity by transmitting more information in the amplitude, phase, polarization or a combination of all. The BS front-end comprises of the 60 GHz upconverter and a 60 GHz planar  $2 \times 2$  microstrip antenna. The 10 GHz IF carrier allows an optical transmission with higher spectral efficiency in optical domain, as well as it is less susceptible to dispersion induced power fading inherent in optical fiber. Characterization of the designed central station and base station front-end through measurements are presented and discussed. The IF-over-Fiber system analysis is made for the 2 Gbps QPSK transmission with respect to error vector magnitude (EVM), eye and constellation diagrams.

# Zusammenfassung

Die Nachfrage nach kleinen und portablen elektronischen Geräten hat dazu beigetragen, dass unter Nutzung von miniaturisierten Leiterplatten kompakte eingebettete Systeme realisiert werden. Im kommerziellen Markt gibt es einen großen Wettbewerb um kleinere und leichtere Elektronik bei Anwendergeräten im Medizin-, Kommunikations- und Automobilbereich. Die Möglichkeiten, kostengünstige elektronische Komponenten in planarer Technologie zu integrieren, hat zu unterschiedlichen Ansätzen im Entwurf und der Fertigung kompakter Einheiten geführt.

In dieser Arbeit wurden ein Zentralstations- und ein Basisstationsfrontend mit kleinem Formfaktor durch die Nutzung kommerzieller Komponenten auf Leiterplatten realisiert. Diese kompakten elektronischen Einheiten wurden in die IF-over-Fiber-Architektur integriert. Diese IF-over-Fiber-Architektur ist aufgebaut aus miniaturisierten elektronischen Komponenten für Quadratur-Modulation und Aufwärtsmischung. Die Zentralstation unterstützt Modulationen mit Multi-Gbps Datenrate, um die spektrale Effizienz der übertragenen Information zu erhöhen. Multi-Level-Modulationsformate werden in Betracht gezogen und können die Übertragungskapazität verdoppeln, indem mehr Information in der Amplitude, Phase, Polarisation oder einer Kombination von allem übertragen wird. Das Basisstations-Frontend besteht aus dem 60 GHz Aufwärtsmischer und einer planaren 2x2 60 GHz Mikrostreifenantenne. Der 10 GHz Zwischenfrequenzträger erlaubt eine optische Übertragung mit hoher spektraler Effizienz im Optischen und ist auch weniger anfällig gegenüber dispersionsbedingten Leistungsschwankungen, die durch die optische Faser verursacht werden. Die Charakterisierung der entworfenen Zentralstation und des Basisstationsfrontends wird mittels Messungen vorgestellt und diskutiert. Die Systemanalyse des IF-over-Fiber-Systems wird anhand einer 2 Gbps QPSK-Übertragung bezüglich Error Vector Magnitude (EVM), Augen- und Konstellationsdiagrammen vorgenommen.

# Contents

<b>Abstract</b>	<b>ii</b>
<b>Zusammenfassung</b>	<b>iii</b>
<b>Contents</b>	<b>iv</b>
<b>List of Figures</b>	<b>vii</b>
<b>List of Tables</b>	<b>xiii</b>
<b>Acronyms</b>	<b>xiv</b>
<b>List of Symbols</b>	<b>xvii</b>
<b>1 Introduction</b>	<b>2</b>
1.1 Evolution of Access Technology . . . . .	5
1.2 Mobile Broadband Capacity Demand . . . . .	7
1.3 RoF Technology for Seamless Indoor Wireless Communication . . . . .	8
1.4 Objectives and Synopsis of the Dissertation . . . . .	10
<b>2 Basics of Microwave Photonics</b>	<b>12</b>
2.1 Components of a RoF Transmission Link . . . . .	13
2.1.1 Light Source . . . . .	13
2.1.2 E\O Conversion . . . . .	15
2.1.2.1 Direct Modulated Laser (DML) . . . . .	16
2.1.2.2 Electro-Absorption Modulator (EAM) . . . . .	17
2.1.2.3 Mach-Zehnder Modulator (MZM) . . . . .	18
2.1.3 O\E Conversion . . . . .	21
2.1.4 Electronic Components . . . . .	26
2.1.4.1 RF Mixer . . . . .	26
2.1.4.2 I/Q Modulation . . . . .	28
2.2 Transmission Medium . . . . .	30
2.2.1 Optical Fiber Communication . . . . .	31
2.2.1.1 Optical Channel . . . . .	32
2.2.2 Wireless Channel . . . . .	38
2.2.2.1 Frequency Allocation and Planning . . . . .	39
2.3 RoF System Approaches . . . . .	40
2.3.1 Analogue or Digital Modulation? . . . . .	40
2.3.2 Analogue Optical Modulation Techniques . . . . .	42

2.3.2.1	Electrical Signal Generation . . . . .	42
2.3.2.2	Hybrid Carrier . . . . .	44
2.3.3	Radio over Fiber Link Architectures . . . . .	46
2.3.3.1	RF-over-Fiber System . . . . .	49
2.3.3.2	IF-over-Fiber System . . . . .	53
<b>3</b>	<b>IFoF System Design</b>	<b>56</b>
3.1	System Architecture . . . . .	56
3.1.1	Spectral Efficiency . . . . .	58
3.1.2	Electrical Bandwidth . . . . .	60
3.1.2.1	Relative Mixer Bandwidth . . . . .	61
3.1.3	Optical Bandwidth . . . . .	62
3.2	IFoF Link Design Requirements . . . . .	66
3.2.1	Carrier Frequency . . . . .	67
3.2.2	Light Source . . . . .	67
3.2.3	Wireless Link Budget at 60 GHz . . . . .	68
3.2.4	Antenna Design . . . . .	71
3.2.5	Form Factor . . . . .	72
3.2.6	Cost and Simplicity . . . . .	73
<b>4</b>	<b>Central Station</b>	<b>75</b>
4.1	Designing, Assembling and Fabricating . . . . .	76
4.1.1	Choice of RF Components . . . . .	76
4.1.2	DC Biasing Circuits . . . . .	79
4.1.3	PCB Fabrication and Layout . . . . .	81
4.2	Central Station Measurements . . . . .	85
4.2.1	Electronic IQ Modulator Characterization . . . . .	85
4.2.1.1	Conversion Gain . . . . .	87
4.2.1.2	Port Isolation . . . . .	89
4.2.1.3	Phase Noise . . . . .	91
4.2.2	Power Amplifier . . . . .	92
4.3	Central Station Demonstrator . . . . .	96
4.3.1	Optical Intensity Modulation . . . . .	97
4.3.2	Direct Intensity Detection . . . . .	98
<b>5</b>	<b>Base Station Front-end</b>	<b>102</b>
5.1	Designing, Assembling and Fabricating . . . . .	103
5.1.1	Choice of RF Components . . . . .	103
5.1.2	60 GHz Wireless Antenna at BS . . . . .	108
5.1.3	DC Biasing Circuits and PCB Layout . . . . .	112
5.1.3.1	Stepped-Impedance Low-pass Filter . . . . .	116

5.2	The BS Front-end Characterization . . . . .	118
5.2.1	PCB Measurements . . . . .	120
5.2.1.1	10 GHz IF Input . . . . .	121
5.2.1.2	HMC578LC3B x2 Active Frequency Multiplier	123
5.2.2	60 GHz Antenna Array . . . . .	126
5.2.2.1	Far-Field Pattern Analysis . . . . .	128
5.2.3	The Hybrid BS Front-end . . . . .	130
<b>6</b>	<b>System Experiments</b>	<b>134</b>
6.1	Digital Signal Processing . . . . .	134
6.1.1	Offline Digital Filtering . . . . .	135
6.1.2	QPSK Demodulation . . . . .	136
6.1.3	Feedback Timing Correction . . . . .	137
6.1.3.1	Matched Filter . . . . .	139
6.1.3.2	Timing Error Estimation . . . . .	140
6.1.4	Carrier Recovery . . . . .	143
6.1.4.1	Decision-Direct Carrier Recovery Loop . . . . .	143
6.2	Characterization of the Link with the 10 GHz IFoF . . . . .	145
6.2.1	The Error Vector Magnitude . . . . .	146
6.2.1.1	Linking EVM, BER and SNR . . . . .	147
6.2.2	Back-to-Back Performance . . . . .	148
6.2.3	Over Single Mode Fiber (SMF) Span . . . . .	151
6.3	The 60 GHz Fiber-Wireless RoF Link . . . . .	154
6.3.1	Upconversion of Millimeter Wave Carriers . . . . .	156
<b>7</b>	<b>Conclusion and Outlook</b>	<b>158</b>
7.1	Conclusion . . . . .	158
7.2	Outlook . . . . .	159
	<b>Bibliography</b>	<b>162</b>



# List of Figures

1.1	Attenuation characteristics of a typical optical fiber [98]. . . . .	3
1.2	Evolution of access technology. . . . .	6
1.3	An increasing gap between traffic and operator's income (data from [50]). . . . .	7
1.4	Indoor deployment of wireless networking at 60 GHz. . . . .	9
2.1	Schematic highlight of the fundamental concept of analogue microwave photonic link consisting of uplink (from wireless user to BS to CS) and downlink (CS to BS to the wireless user). . . . .	12
2.2	Input current vs output optical power (L-I) curve [32]. . . . .	16
2.3	E\O conversion (dashed lines) using basic intensity modulation techniques. . . . .	17
2.4	Transfer characteristics of: (a) EAMs and (b) MZMs [169]. . . . .	18
2.5	Optical fields propagation within MZM [111]. . . . .	19
2.6	PD linear responsivity curve. . . . .	21
2.7	Responsivity curves of a photodetector depending on its composition as a function of wavelength [46]. . . . .	22
2.8	Techniques used in photo-detection (a) Direct photo-detection and (b) Coherent photo-detection [160]. . . . .	23
2.9	BER as a function of SNR for coherent and direct detection techniques. . . . .	25
2.10	RF mixer for (a) upconversion (b) downconversion. . . . .	27
2.11	I/Q Modulator. . . . .	28
2.12	The in-phase channel, quadrature channel and the QPSK modulated carrier for the data sequence 00011110. . . . .	30
2.13	Fiber dispersion-induced power fading for an ideal optical system employing ODSB modulation as a function of (a) fiber length for SMF (b) RF carrier frequency for SMF. . . . .	34
2.14	Optical sideband modulation shemes for a (a) double sideband (b) single sideband and (c) double sideband suppressed carrier. . . . .	36
2.15	Calculated free space path loss as a function of link distance $d_0$ with respect to carrier frequency. . . . .	39
2.16	Channelization of the 60 GHz in Europe on the left and world-wide spectrum availability on the right [80]. . . . .	40
2.17	Block diagram of (a) the information source and (b) the electrical signal generation. . . . .	43
2.18	MZM optical signal characterization. . . . .	45

2.19	Different schemes for signal modulation on the optical carrier for (a) BB over Fiber (b) IF over Fiber and (c) RF over Fiber.	47
2.20	Effects of chromatic dispersion with transmission distance for 1 dB induced C/N penalty.	49
2.21	Multi-channel transmission scenario consisting of point-to-multipoint RoF links with WDM [91].	51
3.1	Diagrammatic representation of the external modulated IFoF link with IM/DD and upconversion, showing only electrical and optical carriers.	57
3.2	Constellation diagrams of BPSK, QPSK, 8-PSK, and 16-QAM modulation formats.	60
3.3	IQ mixer real bandwidth	61
3.4	Real IQ mixer bandwidths w.r.t different carrier frequencies.	63
3.5	Baseband (digital) signal spectrums	64
3.6	RoF ODSB modulation	64
3.7	Spectral efficiency of RoF system w.r.t relative bandwidth.	65
3.8	Theoretical spectral efficiencies of a 10 GHz carrier with 5 Gbps data rate for optical transmission systems w.r.t baseband and analogue RoF.	65
4.1	Electronic IQ modulator schematic design.	75
4.2	Simulated 10 GHz carrier modulated by the electronic IQ modulator for 5 Gbps QPSK transmission data rate.	79
4.3	Simulation of the input impedance of the decoupling circuit network for the IQ mixer, RF amplifier, in-phase and quadrature power inputs.	80
4.4	Comparison of the PCB substrate materials dielectric losses: RO4350 and Isola I-Tera.	82
4.5	Simulated microstrip line losses on the Isola Itera substrate material of 0.254 mm height and copper thickness of 35 $\mu\text{m}$ .	83
4.6	4-layer PCB stack-up fabrication with Isola Itera substrate.	84
4.7	Electronic IQ modulator top layer PCB layout.	85
4.8	VNA ports connections and measurements setup.	86
4.9	Photography of the electronic IQ modulator on a 4-layer PCB.	86
4.10	Measured input-output matching of the electronic IQ modulator.	86
4.11	Measured electronic IQ modulator conversion gain.	88
4.12	Schematic diagram of the simulation setup.	88

4.13	Simulated eye diagrams using measurement results obtained in Figure 4.11 with $2^{31}-1$ PRBS sequence. The results are for the 0 dBm LO input power [16] showing clear open eyes up to 3.5 Gbps data rate. . . . .	89
4.14	Electronic IQ modulator isolation measured when input power of -10 dBm was set at in-phase and quadrature inputs and LO at 0 dBm power. . . . .	90
4.15	Measured SSB RF signals with only (a) LSB, and (b) USB for LO: 10 GHz and IF single tone: 2.5 GHz. . . . .	91
4.16	Measured phase noise of the 10 GHz carrier is approx. -120 dBc(1 Hz) at 1 MHz offset. . . . .	92
4.17	Simulated input-output matching of (a) the CC19T40K240G5-C conical broadband inductor, and (b) the 530L104KT broadband capacitor forming the LC network. . . . .	93
4.18	Layout of the circuit design of the power amplifier. . . . .	94
4.19	Comparison between measured and simulated input-output matching for the HMC659LC5 power amplifier. . . . .	95
4.20	Schematic design of IQ upconversion. . . . .	95
4.21	The central station setup for optical and electrical spectral measurements. . . . .	96
4.22	Measured transfer function of the MZM amplitude modulator. . . . .	98
4.23	Measured spectrum of ODSB upconverted modulated signal when the MZM is biased at the quadrature point. . . . .	99
4.24	Comparison between measured spectra of the ODSB at different electrical data rate of 2 Gbps and 7 Gbps, respectively on 10 GHz IF carrier. . . . .	99
4.25	Comparison between the measurements of the electrical transmitted 2.5 Gbps QPSK signal on 10 GHz carrier (CS) and the one detected at the BS when connected B2B and with 2 km SMF. . . . .	100
4.26	Comparison between measured spectra at different data rate of 2 Gbps and 7 Gbps respectively, on 10 GHz IF carrier. . . . .	101
5.1	The schematic of the 60 GHz upconversion. . . . .	103
5.2	$2 \times 2$ microstrip antenna array. . . . .	110
5.3	Simulation results of the input matching and radiation patterns at 60 GHz of the $2 \times 2$ antenna array. . . . .	110
5.4	The footprint of the designed CPW to MS transition with its input-output characteristics. . . . .	111
5.5	The schematic design of the BS on Isola I-Tera MT PCB . . . . .	112

5.6	PCB top layer assembly showing signal routing on other layers as well as the marked position of the silica wafer mounting. . . . .	113
5.7	The schematic design of the BS on fused silica substrate . . . . .	114
5.8	Design and layout on the fused silica substrate. . . . .	115
5.9	Topology of the BS with integrated planar 2×2 antenna array	115
5.10	Equivalent circuit diagrams for stepped-impedance filter. . . . .	116
5.11	Design of the stepped-impedance BPF. . . . .	117
5.12	Simulation result of 25 GHz lumped-elements BPF compensating for the inductive parasitic effects of wire bonding. . . . .	118
5.13	The CPW layout of multiline TRL calibration with custom calibration structures on the glass substrate. The calibration structures are included multiple times to give provision of multiple measurements and counter wearing off of the contact pads.	119
5.14	Overview of TRL calibration of the glass substrate using HF probes on a wafer prober. . . . .	120
5.15	The 2-layer PCB with surface mounting SMPM connectors. . . . .	121
5.16	Photography of the Isola Itera BS measurements using the surface mounted SMPM connectors. . . . .	121
5.17	10 GHz IF input signal characterization. . . . .	122
5.18	S-Parameter simulation of the MAAD-011021 digital attenuator.	122
5.19	Measured input and output matching of the ×2 RF multiplier HMC578LC3B (a) using the SMA edge connector and (b) using the SMPM connector. . . . .	123
5.20	Measured output power of the 2 <sup>nd</sup> harmonic frequency when input power is varied from 3 dBm to -5 dBm . . . . .	124
5.21	Measured isolation of the ×2 RF multiplier HMC578LC3B (a) at 1 dBm drive power and (b) at 3 dBm drive power. . . . .	125
5.22	Measured spectrum of the 1 <sup>st</sup> and 2 <sup>nd</sup> harmonics of the ×2 RF multiplier HMC578LC3B in which at 1 dBm drive level and depicting isolation of -24 dBm, whereas at 3 dBm drive level and depicting isolation of -32 dBm. . . . .	125
5.23	Schematic diagram of the measurement setup. . . . .	127
5.24	Overview of the AUT gain measurement at the middle of the chuck on wafer probing station with receiving horn antenna positioned on top. No absorbers were used in the far-field measurement. . . . .	127
5.25	Comparison between the measured and simulated results of the antenna array with the CPW to MS transition feeding element. . . . .	128

5.26	The effect of probe reflections in far-field pattern measurements showing maxima and minima depending on the path difference [41]. . . . .	129
5.27	Photography of the hybrid BS front-end fabrication. . . . .	131
5.28	Overview of the hybrid BS radiated power measurements using the receiving horn antenna at 13 cm configured through the 67 GHz VNA. . . . .	132
5.29	Measured EIRP of the BS front-end using motor-driven receiving horn antenna at 13 cm connected to the VNA. The gold wafer chuck was covered with absorbers. . . . .	133
5.30	Measured EIRP of the BS front-end in the x- and y-directions using the horn antenna at 13 cm connected to the VNA. . . . .	133
6.1	Comparison between the two filters to demonstrate zero-phase delay filter. . . . .	136
6.2	Spectra of the electrical 2 GHz carrier with 2 Gbps QPSK data captured by DSO at a sampling frequency of 20 Gsa/s. . . . .	136
6.3	Spectral of the digital I/Q demodulator. . . . .	138
6.4	Clock tracking PLL algorithm implemented using Matlab Simulink.	139
6.5	Square root raised cosine filter over 8 symbols with $4\times$ up-sampling and roll-off factor $\beta = 0.5$ . . . . .	140
6.6	Timing recovery fractional delay, $\mu$ during the reception with carrier and timing frequency offset. . . . .	142
6.7	Block diagram of decision-direct carrier recovery loop. . . . .	144
6.8	Carrier phase rotation during reception with carrier and timing frequency offset . . . . .	144
6.9	Received constellation point $M'$ compared to the ideal constellation point $M$ . . . . .	145
6.10	Variation of EVM with SNR. . . . .	147
6.11	Experimental setup testing the 2 Gbps QPSK signal at 10 GHz IF carrier. . . . .	149
6.12	$2\times 500$ Mbps spectra at the output of the EVALZ-ADN2915, with the real part of the generated QPSK baseband signal on the left and the imaginary part on the right. . . . .	149
6.13	Constellation diagrams of 2 Gbps QPSK (a) electrical drive signal for the MZM (b) signal received by the photodiode in B-2-B scenario. . . . .	150
6.14	I and Q eye diagrams: (a) electrical drive signal for the MZM (b) signal received by the photodiode in B-2-B scenario. . . . .	150
6.15	Constellation diagrams of 2 Gbps QPSK with different fiber lengths. . . . .	151

6.16	2 km SMF: I and Q eye diagrams of the 2 Gbps QPSK signal. . . . .	152
6.17	12.8 km SMF: I and Q eye diagrams of the 2 Gbps QPSK signal. . . . .	152
6.18	25.6 km SMF: I and Q eye diagrams of the 2 Gbps QPSK signal. . . . .	152
6.19	Measured EVM (rms) curves for the downlink 2 Gbps QPSK as a function of received optical power (ROP) by the photodiode. . . . .	153
6.20	Experimental setups of the 60 GHz fiber-wireless RoF architecture using intensity modulation and direct detection technique for downlink transmission with data recovery scheme. . . . .	154
6.21	Measured spectra with and without optical link of the up-converted 60 GHz carrier both modulated with 2 Gbps QPSK (VBW, RBW = 3 kHz). . . . .	155
6.22	Spectra of the 59 GHz, 60 GHz and 61 GHz carriers generated by the BS (ESA) (VBW, RBW = 3 kHz). . . . .	157
7.1	A 3D exemplar of compact integrated optoelectronics in a single-package [116]. . . . .	160

# List of Tables

2.1	Comparison between analogue RoF and digital RoF . . . . .	41
3.1	Parameters of the downlink using IM/DD technique . . . . .	59
3.2	Relative mixer bandwidths w.r.t different carrier frequencies . . . . .	62
3.3	Components and parameters used in the noise figure calculation of the wireless system . . . . .	69
4.1	IQ mixer description properties [16, 9, 25] chosen is bolded. . . . .	77
4.2	LNAs properties for the in-phase and quadrature inputs of the IQ mixer [14, 7, 22]. The choice made is bolded. . . . .	78
4.3	Fixed parameters of the microstrip line . . . . .	82
5.1	60 GHz RF mixer description properties [19, 20, 3], in bold the one chosen. . . . .	104
5.2	Available choices for the LNAs and their properties for the IF bandwidth [17, 26] . . . . .	105
5.3	Available choices for the $\times 2$ frequency multipliers and their properties at 12.5 GHz LO input [28, 13, 12]. The isolation of $1F_o$ and $3F_o$ are with respect to the output level. . . . .	106
5.4	The available choices for the $\times 2$ frequency multipliers and their properties at 25 GHz LO input [21, 5]. The isolation of $1F_o$ and $3F_o$ are with respect to the output level. . . . .	107

# Acronyms

<b>ADC</b>	Analogue-to-Digital Converter
<b>AM</b>	Amplitude Modulation
<b>ASE</b>	Amplified Spontaneous Emission
<b>AUT</b>	Antenna Under Test
<b>BBoF</b>	Baseband-over-Fiber
<b>BER</b>	Bit-Error Rate
<b>BPF</b>	Band Pass Filter
<b>BRS</b>	Broadband Radio Service
<b>BS</b>	Base Station
<b>CERRE</b>	Centre on Regulation in Europe
<b>CNR</b>	Carrier-to-Noise Ratio
<b>COTS</b>	Commercial Off-the-Shelf
<b>CS</b>	Central Station
<b>CW</b>	Continuous-Wave
<b>DAS</b>	Distributed Antenna System
<b>DCF</b>	Dispersion Compensating Fiber
<b>DFB Laser</b>	Distributed Feedback Laser
<b>DML</b>	Direct Modulated Laser
<b>DSL</b>	Digital Subscriber Line
<b>DSO</b>	Digital Storage Oscilloscope
<b>EAM</b>	Electro-Absorption Modulator
<b>ECL</b>	External Cavity Laser
<b>EDFA</b>	Erbium Doped Fiber Amplifier
<b>EIRP</b>	Equivalent Isotropically Radiated Power
<b>ER</b>	Extinction Ratio
<b>ESA</b>	Electrical Spectrum Analyser
<b>EVM</b>	Error Vector Magnitude
<b>RF</b>	Radio Frequency
<b>RoF</b>	Radio-over-Fiber
<b>FSO</b>	Free Space Optical
<b>FTTH</b>	Fiber-to-the-Home
<b>FTTA</b>	Fiber-to-the-Antenna
<b>FWM</b>	Four-Wave Mixing
<b>GVD</b>	Group Velocity Dispersion
<b>IC</b>	Integrated Circuit
<b>IF</b>	Intermediate Frequency
<b>IFoF</b>	IF-over-Fiber
<b>IIR</b>	Infinite Impulse Response



*List of Tables*

---

<b>IM</b>	Intensity Modulation
<b>IM-DD</b>	Intensity Modulation Direct Detection
<b>IQ</b>	In-phase and Quadrature
<b>ISI</b>	Inter Symbol Interference
<b>ISM</b>	Industrial, Scientific and Medical
<b>LED</b>	Light-Emitting Diode
<b>LMDS</b>	Local Multipoint Distribution Service
<b>LO</b>	Local Oscillator
<b>LOS</b>	Line-of-Site
<b>LSB</b>	Lower Sideband
<b>MATP</b>	Maximum Point
<b>MITP</b>	Minimum Point
<b>ML</b>	Maximum Likelihood
<b>MMF</b>	Multi-Mode Fiber
<b>M-PSK</b>	M-ary Phase Shifting Keying
<b>M-QAM</b>	M-ary Quadrature Amplitude Modulation
<b>MS</b>	Mobile Station
<b>MZM</b>	Mach-Zehnder Modulator
<b>NCO</b>	Numerical Controlled Oscillator
<b>NF</b>	Noise Figure
<b>NGA</b>	Next Generation Access
<b>NRZ</b>	Non-Return to Zero
<b>NRZ-OOK</b>	Non-Return-to-Zero-on-off-Keying
<b>OCSR</b>	Optical Carrier-to-Side Ratio
<b>ODSB</b>	Optical Double Sideband
<b>ODSB-SC</b>	Optical Double Sideband Suppressed-Carrier
<b>OSSB</b>	Optical Single Sideband
<b>PA</b>	Power Amplifier
<b>PC</b>	Polarization Controller
<b>PCB</b>	Printed Circuit Board
<b>PD</b>	Photodetector
<b>PLL</b>	Phase Locked Loop
<b>PON</b>	Passive Optical Network
<b>PRBS</b>	Pseudo-Random Sequence
<b>PTMP</b>	Point-to-Multipoint
<b>QAM</b>	Quadrature Amplitude Modulation
<b>QP</b>	Quadrature Point
<b>QPSK</b>	Quadrature Phase Shift Keying
<b>RFoF</b>	RF-over-Fiber
<b>RIN</b>	Relative Intensity Noise
<b>ROP</b>	Received Optical Power

*List of Tables*

---

<b>RZ</b>	Return to Zero
<b>SBS</b>	Stimulated Brillouin Scattering
<b>SCM</b>	Sub-Carrier Multiplexing
<b>SFDR</b>	Spurious Free Dynamic Range
<b>SMA</b>	SubMiniature version A
<b>SMF</b>	Single-Mode Fiber
<b>SNR</b>	Signal-to-Noise Ratio
<b>SPM</b>	Self-Phase Modulation
<b>SRS</b>	Stimulated Raman Scattering
<b>TDM</b>	Time-Division Multiplexing
<b>TRL</b>	Thru Reflect Line
<b>USB</b>	Upper Sideband
<b>UTC-PD</b>	Uni-Travelling-Carrier Photodiode
<b>VCO</b>	Voltage Controlled Oscillator
<b>VCSEL</b>	Vertical-Cavity Surface-Emitting Laser
<b>VNA</b>	Vector Network Analyzer
<b>WDM</b>	Wavelength-Division Multiplexing
<b>WPAN</b>	Wireless Personal Area Network
<b>XPM</b>	Cross-Phase Modulation

# List of Symbols

$I$	Current
$E$	Electric field
$P$	Power
$P_{MAX}$	Maximum RF input power
$P_{TX}$	Transmitted RF power
$P_{RX}$	Received RF Power
$\omega$	Angular frequency
$\omega_C$	Cut-off frequency
$\varphi$	Angular phase
$\delta P(t)$	Laser intensity fluctuation
$V_\pi$	Modulation extinction voltage
$P_{bias}$	Modulator normalized bias
$\delta$	Modulator normalized bias
$\beta$	Modulator normalized index
$R$	Responsivity of photodiode
$\hbar$	Planck's constant
$\hbar v$	Photon energy
$k$	Boltzmann's constant
$\lambda_c$	Carrier wavelength
$c$	Speed of light in vacuum
$q$	Electron charge
$f_c$	Carrier frequency
$E_b$	Energy per symbol
$E_g$	Bandgap of the semiconductor material
$\tilde{N}_0$	Noise power spectral density
$C$	Channel capacity
$M$	Number of bits per symbol
$T$	Symbol period
$\zeta(t)$	Dirac delta function
$T_s$	Sample period
$n_s$	Number of registers
$\alpha$	Attenuation constant
$L$	Fiber length
$D$	Fiber dispersion constant
$\chi_\sigma$	Shadowing and multi-path fading effects parameter
$\tilde{n}$	Path loss exponent
$B$	Bandwidth
$B_{Sign}$	RF signal bandwidth

List of Tables

---

$B_{Optical}$	Optical signal bandwidth
$J_n$	Bessel function of the $n^{th}$ order
$d$	Distance
$d_0$	Reference distance
$\eta_{TX}$	Laser slope efficiency
$\eta_{RX}$	Photodiode responsivity
$Z_{in}$	Input impedance
$Z_{out}$	Output impedance
$Z_w$	Microstrip impedance
$F$	Noise factor
$NF$	Noise figure
$G$	Gain
$G_{RoF}$	Radio over fiber link gain
$G_{RX}$	Receiving antenna gain
$G_{conv}$	Conversion gain
$G_{AUT}$	Antenna gain under test
$\hat{G}_{horn}$	Horn antenna gain
$PL$	Path loss
$PL_{FS}(d_0)$	Path loss of the reference distance
$\alpha_{dielectric}$	Material dielectric loss
$\alpha_{conduction}$	Material dielectric loss
$\tan \delta$	Material dispersion factor
$\varepsilon_r$	Material dielectric constant
$\varepsilon_0$	Dielectric constant of free space
$H$	Substrate material height
$\theta$	Carrier phase offset
$w$	Microstrip trace width
$\epsilon$	Symbol timing error
$P_b$	Bit error probability
$\mu$	Fractional time delay

# 1

## Introduction

The enormous capacity offered by the optical fiber, combined with the mobility and the seamless flexibility of wireless access, developed to what is known today as radio-over-fiber (RoF) technology. RoF based optical-wireless networks are emerging as cost-effective solutions in environments where seamless connections are needed, such as in conference centers, railways, airports, hotels, homes and small offices [81, 95, 130, 166]. Advances in RF and microwave circuitry go hand in hand with everyday evolution in technology. A large portion of these innovations consist of bandwidth-intensive applications on hand-held wireless devices for medical, industrial, and communicational applications. These applications in a variety of fields are migrating from desktop models to portable communication units [112, 121]. This induced undeniable demand for data-rates boosted beyond 10 Gbps with no end in sight, calls for system architectures that support multi-Gbps data modulation schemes to increase spectral efficiency of transmitted signal. Not only is RF becoming more ubiquitous, but also microwave circuitry. Both capturing very high frequencies in millimeter wavelength within the frequency spectrum from 30 GHz to 300 GHz. For indoor deployments and applications, the research interest is now on the 60 GHz bands [71, 132].

The fundamental principle of RoF transmission is that it requires a transportation of analogue radio signals through an optical fiber link. This is because the optical source is always operated in “on” state and the optical modulation depth is so small that small signal analysis of the various link devices is possible. In contrast to digital optical links, the optical modulation depth approaches almost 100% [66], whereby, the laser is operated in the “on” and “off” states depending on the modulating data sequence. Compared to copper cables, the loss in the optical fiber is a function of the optical wavelength shown in Figure 1.1 and does not depend on the frequency of the RF signal being transported. The C-Band and L-Band windows have minimum losses in the wavelength ranging from 1.53  $\mu\text{m}$  to 1.625  $\mu\text{m}$ .

For standard single mode fibers, the loss of this transmission distance due to the fiber attenuation is 0.2 dB/km at the wavelength of 1550 nm, see Figure 1.1. The chromatic dispersion effect introduces distortions of the signal. It

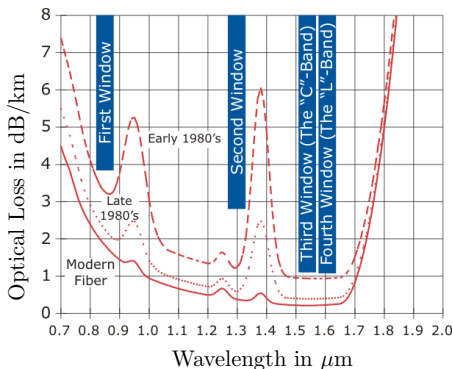


Figure 1.1: Attenuation characteristics of a typical optical fiber [98].

has been shown in [74] that for a standard single mode fiber with a chromatic dispersion of 17 ps/km-nm and a length of 1 km, the SNR-penalty induced by the fiber dispersion for a signal frequency of 30 GHz is less than 1 dB. The effect is even less prominent for lower signal frequencies, which is the interest of investigation in this dissertation. Consequently, due to the abundant bandwidth and frequency-independent low-loss properties, multiple RF carriers can be multiplexed and transmitted via a single mode optical fiber. These are the techniques used for long haul undersea optical transmission systems [66].

For system simplicity, cost-efficient and low-maintenance high-performance links, analogue intermediate frequency (IF) or radio frequency (RF) signal over fiber systems is preferred [57]. Conversely, nonlinear distortions, limited dynamic range, and additional noise are introduced to the transmitted signal. One approach to mitigate these induced signal impairments is to use digitized IF or RF signal over fiber from the central station (CS) to the base station (BS). Digitalized transmission (I and Q baseband) consumes more capacity than analogue transmission, and increases system complexity and cost; as it requires signal conversion prior and after transmission over fiber. Moreover, for analogue optical links, the propagation delay is simply given by the speed of light in the fiber and the fiber length; contrarily, in digital links, additional delays are typically acquired in the digitization process. Optical techniques at the CS have traditionally been used to generate stable signals over a wide range of frequencies, employing a variety of methods such as direct modulation, external modulation, mode-locking and optical hetero-

dyning [66]. Usually, in typical analogue optical fiber links, signal distortion is caused mainly by the modulating device, rather than the photodetector or the fiber. Once the CS has to be connected to the multiple distributed antenna system (DAS), multiplexing techniques are implemented to reduce the number of optical fiber counts. The progress in the development of optical components enables the design of a RoF system capable of transporting RF signals with advanced multilevel modulation formats over significant distances, thereby enabling its use in any next generation DAS network. A combination of wavelength and subcarrier multiplexing is the most convenient method in analogue RoF links. In digitized RoF links, time-division multiplexing (TDM) with combination of wavelength division-multiplexing (WDM) is often applied for long haul transmission [66].

In the RoF system design, the rule of thumb is selecting appropriate technologies for each subsystem with a goal of reducing capital and operational expenses of the network [38]. At the CS, high frequency electro-optical modulators and electronics have to be avoided due to their high cost [122] and power consumption [159]. Concurrently, complex implementation of downlink transmission techniques are also not preferred because they result in higher manufacturing and maintenance costs. The cost of the optical link is mainly determined by the fiber installation rather than by the optical components. Thus, integrating optical segments into hybrid solutions (fiber sharing) for the next generation of access networks is a key measure for reducing cost. However, it is important to minimize fiber length because topologies with minimum fiber lengths often offer poor availability performance [47]. Regarding the BS, it is critical to keep it as simple as possible because an elevated number of them are required in the RoF system, meaning a BS with the lowest possible number of components. The simplicity of the BSs, drives the reduction of costs associated with site acquisition, site leasing and energy consumption. It is desirable for the BS to work without any expensive climate control facilities at the remote site [38]. On the other hand, as a classical downsizing technique, miniaturization attempts have been performed using different types of the substrate material. The existing RoF systems are huge and bulky with large transmitting antenna at the BS, which render their mass production inconceivable. On the contrary, using printed circuit board (PCB) technology to converge the electrical components of the system into a compact unit is realistic. The challenge is taken to design and assemble electrical components and microwave circuitry of the analogue RoF on PCB.

## 1.1 Evolution of Access Technology

The chronicle of access technology commences with copper cables. The use of copper cables traces way back to the beginning of the 19th century, where text and voice were the main content for transmission. Discovery of mobile phones by Motorola in 1973 promoted growth in the access network. Subsequently, ten years later, handheld mobile phones named “DynaTAC 8000x” became commercial. Mobile voice and text messages were amazing, although consumers wanted more. Consumers were later introduced to broadband internet access in the homes and offices. From 1983 to 2010s, mobile networks evolved through four generations with insatiable demand for broadband bandwidth and data services. Thanks to the second generation (2G) of mobile networks which enabled more users to acquire mobile subscriptions. Innovations in device technology resulted in the era of the smartphone. The proliferation of smartphones paved the way for networks of wireless connectivity on top of secure wired backbones linking base stations to the overall global communications network. The wireless infrastructure is essentially always a hybrid of wired and wireless, which offers a completely different level of flexibility and access compared to wired-only network infrastructure.

Fiber optics inherently have huge bandwidth and offer higher data rates than copper cables. They are immune to electromagnetic interference and have a low bit error rate. Although copper cables are already installed for telephone signals and cable television services, fiber optics cables can reach longer distances and facilitate data rates beyond 1 Gbps. The fiber cable installation for copper cable replacement has been conceived in many countries, albeit proved to be far more expensive. In the beginning, this concept was implemented to cover small distances in the communication network, abbreviated to FTTx meaning fiber-to-the-x, where x defines end users configurations for fiber deployment. In many instances, FTTH (fiber-to-the-home) has become a standard choice for fiber utilization in greenfield areas [51]. In addition, many countries have embarked on new big fiber installation projects interconnecting cities and remote centers. Most of the telecommunication companies are currently using fiber optics for long-distance communication. Repeaters are required at distance intervals to amplify and preserve transmitted signal contents. Beyond imagination, fiber is now explored for space and cloud radio access widely referred to as free space optical (FSO) communication.

FSO systems have initially attracted attention as an efficient solution to the “last mile” problem to bridge the gap between the end user and the fiber optic infrastructure already in place. Unlike RF carrier where spectrum usage is restricted, optical carrier does not require any spectrum licensing. As a result it is an attractive prospect for high bandwidth and capacity applications.



Contrary to its great potential, the performance of FSO communication is limited by the atmospheric channel effects of absorption, scattering and turbulence. Different communication protocols were developed [99, 97], and FSO communication is considered as a candidate for 5G backhaul [65].

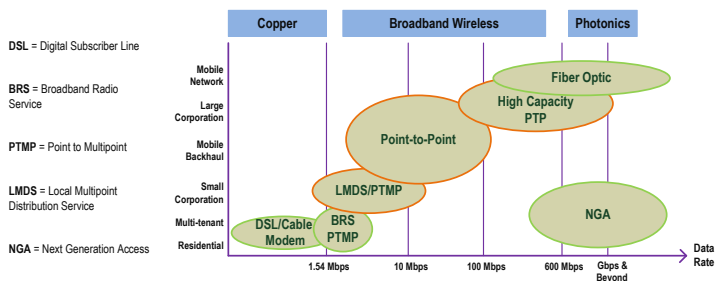


Figure 1.2: Evolution of access technology.

Access technology evolution enables varying Gbps data rate experiences and beyond; as depicted in Figure 1.2. Still, many households in Europe await the next generation access (NGA) networks according to the Centre on Regulation in Europe (CERRE) report on “State aid for broadband infrastructures in Europe” released in 2018 [119]. NGA technologies have low share in fixed broadband lines with an increase in data rates and quality of service. In order to achieve the transmission of such higher data rates, systems with high spectral efficiencies beyond 10 bit/s/Hz have to be developed, which will be very challenging. The simultaneous multi-channel transmission has been employed to attain such higher spectral efficiency of the transmitted signals. Standardized systems with transmission data rates of 2.5 Gbps, 10 Gbps, 40 Gbps, 100 Gbps and 200 Gbps are operational and commercial. Besides, quadrature modulation is desired for its ability to accommodate more transmission bits per channel; utilizing both amplitude and phase variations of the transmitted data signal.

Modern optical communication systems fulfilling optical networking functionalities at data rates of about 40 Gbps and above are now commercially available. They employ wavelength division multiplexing (WDM) technique due to the rapid development of high-speed electronics and optical component technologies over the last few years. NGA networks are envisioned to operate at a data rate as high as 400 Gbps.

## 1.2 Mobile Broadband Capacity Demand

Mobile broadband services are undergoing a period of dramatic growth causing a tremendous increase in data traffic. This surge of traffic is driven by the growing number of mobile subscribers, especially smartphone users connecting to faster network applications such as video streaming, full HD video and cloud computing. These applications require wireless data rates of several 10s of Gbps and the real feel of being ubiquitous by mobile subscribers. These bandwidth-hungry applications are highly dependent on the capacity provided by the telecommunication infrastructures. In fact, with a capacity-demand growth doubling every year [50], the paradigm in telecommunication networks has rapidly changed from supporting local and low bandwidth traffic to providing worldwide connections with high bandwidth-consuming traffic. This evolution has been verified in all segments of the telecommunication networks, ranging from the access to the metropolitan and backbone networks, which were forced to cope with larger traffic volumes by upgrading their systems and technologies.

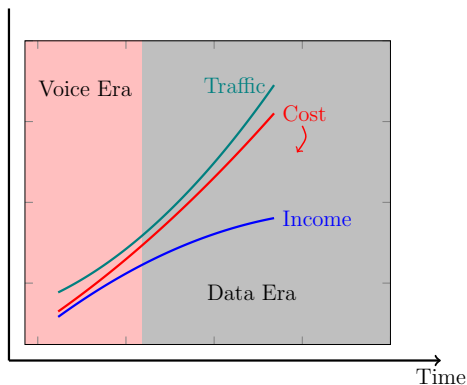


Figure 1.3: An increasing gap between traffic and operator's income (data from [50]).

At present, mobile service operators and the telecommunication industry as a whole, face an important challenge of users expecting high bandwidths, low loading times and reduced latency in real-time services. Telecommunication networks, apart from providing a high transmission capacity also need to be reliable, flexible, fault-tolerant and low energy consuming with ever

decreasing cost per transported bit. As depicted in Figure 1.3, and referred to by many different organizations, mobile operators currently face a growing gap between their income revenues and the increasing traffic demand. This is verified because the increasing expenditures necessary to upgrade the network capacity are typically not supported by proportionally augmenting mobile operator income revenues. In reality, most mobile operators experience a very slow, income revenue increase. Therefore, the present challenge requires new network technologies and architectures which allow upgrading the capacity while simultaneously reducing the cost per transported bit. In order to reduce the telecommunication system cost and provide solution for the increase in mobile traffic demand, RoF technology has been proposed since it supports simple BSs that are interconnected to a CS via an optical fiber. The RoF as part of optical communication system could be one of the solution for the high demand of high speed communication with broad bandwidth. It has been proven to be one of the best integrated optical fiber communication for an indoor high speed transmission system [66, 121].

### 1.3 RoF Technology for Seamless Indoor Wireless Communication

To deliver on this significant wireless system demand, particularly for inbuilt coverage, millimeter wave wireless technology, which is capable of multi-Gbps throughput, is very promising. Progress in the wireless personal area networks (WPAN) from RFID, ZigBee, Bluetooth 2.0, W-USB to 60 GHz wirelessHD appears to be rising at a much faster rate than ordinary wireless technologies [61]. Anyhow, the apparent rapid increase in capacity of WPANs is a clear testimony of the significance of high-speed wireless access for the users, and an introduction of new fast communication networks. These emerging personal wireless communication networks (that support new broadband services) provide increased opportunities for photonics technologies to play a prominent role in the realization of the next generation integrated optical and wireless networks.

RoF transmission has extensively been studied as a means of realizing a fiber optic wireless distribution network that enables seamless integration of the optical and wireless network infrastructures [38, 66, 121, 166]. An unprecedented 7 GHz bandwidth of un-channelized spectrum for operation between 57-64 GHz is available in Europe for ISM (Industrial, Scientific, and Medical) band for RoF systems. This license-free spectrum is exploited due to its enhanced characteristics of point-to-point link transmission with a higher

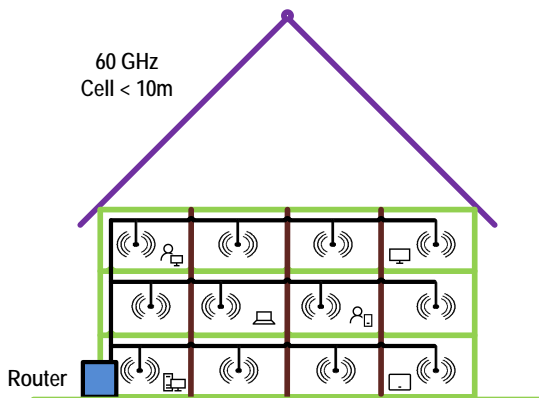


Figure 1.4: Indoor deployment of wireless networking at 60 GHz.

throughput greater than 1 Gbps. A particular strong interest is now on the 60 GHz bands, especially for in-building applications. Nevertheless, these frequencies have an inherent high propagation loss characteristic of wireless signals resulting in network architectures featuring significantly smaller cell sizes. Increasing interest in the use of fiber optic for wireless transmission is stimulated by the ability of the RoF system to support very small antenna transmission sizes of pico and femto dimensions in a confined area (Figure 1.4), which increases transmission throughput and enhance frequency reuse. Yet, deployments of these pico and femto cells require many DAS. Antenna density is required for improved wireless signal coverage and indoors capacity, whereas, poor wireless signal results in wireless system performance degradation. Integrating a 60 GHz wireless system with a fiber optic distribution network enables efficient delivery of high-speed wireless signals to a large number of indoor wireless access points, ensuring optimized radio coverage. Consequently, 60 GHz wireless presents great opportunities for multi-Gbps wireless communication. Even when using only low spectrally efficient basic modulation formats like NRZ-OOK, the capacity of the millimeter wave band already surpasses the capacity of conventional microwave band due to the availability of channel bandwidth.

The RoF transmission is characterized as analogue transmission; owing to the fact that RF signal is used to modulate the lightwave, not a baseband digital signal as it is the case in most optical communication links. The use of the

RF signal means that the link is analogue in nature and its operation must be characterized as such. Analogue RoF architecture can be implemented using RF or IF. The advantage of using IF-over-fiber is the fact that the impinging fiber chromatic dispersion effects are reduced at the expense of additional components for upconverting IF to RF. Power fading due to chromatic dispersion lowers the transmission distance with increasing frequency. As well, distributed feedback (DFB) laser used for lightwave generation and a photodiode at the receiver for lightwave detection and conversion to electrical domain operate at lower frequencies. Certainly, IF-over-Fiber is a good compromise between electrical bandwidth that will be available and component effort. IF instead of RF over fiber enables metro network distances and multiple carrier transmission. This architecture offers flexibility to support system outgrowth and expansion to accommodate new interfaces and components. On the other hand, RF-over-fiber transmission severely suffers from chromatic dispersion effects with the increase in fiber transmission length. Complex techniques in carrier recovery at the receiver have to be employed in order to detect transmitted signal. Therefore, it is not preferred for multichannel transmission over fiber [94].

Fiber-to-the-antenna (FTTA) is a new innovation for broadband network architecture in which optical fiber is used to connect a remote antenna of the BS [176]. FTTA can be seen as a subset of RoF where the optical fiber is brought closer to the transmitting antenna at the BS. This system setup allows for enhanced energy efficiency, increased bandwidth, improved flexibility and low latency which are the defined properties of the NGA network.

## 1.4 Objectives and Synopsis of the Dissertation

Undertaking this research on RoF systems is intended to seek ways of simplifying the system architecture. Designing a RoF transmission system consisting of compact CS and BS units while optimizing electrical component's cost, size and performance. The goal is to explore a compromise between high performance at 60 GHz frequency of WiFi routers available in the market and compact size of the receiver (BS) designed. Therefore, the design and realization of a cost-effective RoF system with improved portability (reduced bulkiness) and high data rate using off-the-shelf RF components is proposed. In addition, the study aims at mitigating optical transmission losses using a transmission carrier at intermediate frequencies.

The study comprises of seven chapters. Basic concepts of microwave photon-

ics in relation to fiber optic communication is introduced and discussed in the next chapter. Intensity and phase (including frequency) data modulation formats are reviewed. This comprises the physical quantity used to convey digital information, and the number of symbols used to represent the binary transmit data. Likewise, the distribution of radio signals over optical fiber to take advantage of the low loss, mitigating chromatic dispersion effects and utilizing broadband bandwidth of the state-of-the-art IF-over-Fiber architecture transmission are reviewed. The intensity of an optical signal is the square of its amplitude, where its detection is carried out using direct envelope detection scheme by a photodetector (PD). Chapter three introduces the system design and criteria for consideration; which are simplicity, affordability, and easy deployment while minimizing insertion loss and system noise. Selection of transmission frequency, RF components and fabrication technology are presented. It shows that the transmission with high linearity for a system consisting of numerous power amplifiers has trade-offs between poor system efficiency and high transmission spectral efficiency. The downlink transmission layout comprising the CS and BS, which are interconnected by optical fiber for electro-optical and optical-electro conversions respectively, have been discussed.

Chapter four is dedicated to the design, fabrication and characterization of the CS on PCB using Isola I-Tera MT substrate material. The CS supports multi-Gbps data modulation schemes in order to increase spectral efficiency of the analogue transmitted signal. Special attention has been given to external laser modulated link using Mach-Zehnder Modulator (MZM) biased at quadrature. RF amplifiers are incorporated in order to drive the MZM into full capacity. Chapter five deals with the BS for wireless transmission at 60 GHz. This consists of design and fabrication of integrated microstrip antenna array transmitting at 60 GHz. At 60 GHz frequency, signal transmission experiences more losses as it crosses the PCB. A proposed hybrid solution of using two substrate materials has been realized using a PCB (Isola I-Tera MT substrate) and a wafer (silica substrate). Thereafter, chapter six focuses on the performance of the IF-RoF link transmission; characterization and experimental results. The dissertation is concluded by chapter seven with commentary and summary of the work and its contribution to the ongoing research on RoF systems.